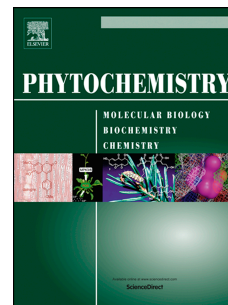


Journal Pre-proof

Bioactivity-guided isolation of trypanocidal coumarins and dihydro-pyranochromones from selected Apiaceae plant species

Sandhya R. Krishnan, Adrianna Skiba, Simon Vlad Luca, Laurence Marcourt, Jean-Luc Wolfender, Krystyna Skalicka-Woźniak, Jürg Gertsch



PII: S0031-9422(23)00186-3

DOI: <https://doi.org/10.1016/j.phytochem.2023.113770>

Reference: PHYTO 113770

To appear in: *Phytochemistry*

Received Date: 28 February 2023

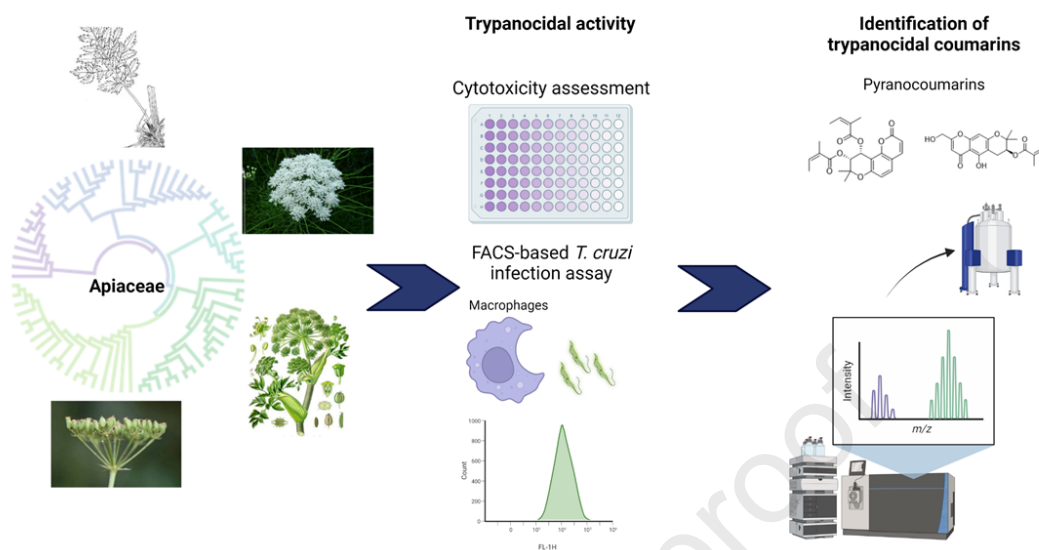
Revised Date: 14 June 2023

Accepted Date: 15 June 2023

Please cite this article as: Krishnan, S.R., Skiba, A., Luca, S.V., Marcourt, L., Wolfender, J.-L., Skalicka-Woźniak, K., Gertsch, J., Bioactivity-guided isolation of trypanocidal coumarins and dihydro-pyranochromones from selected Apiaceae plant species, *Phytochemistry* (2023), doi: <https://doi.org/10.1016/j.phytochem.2023.113770>.

This is a PDF file of an article that has undergone enhancements after acceptance, such as the addition of a cover page and metadata, and formatting for readability, but it is not yet the definitive version of record. This version will undergo additional copyediting, typesetting and review before it is published in its final form, but we are providing this version to give early visibility of the article. Please note that, during the production process, errors may be discovered which could affect the content, and all legal disclaimers that apply to the journal pertain.

© 2023 Published by Elsevier Ltd.



Study on trypanocidal coumarins effective against the parasite *Trypanosoma cruzi* indicated pyranocoumarins and dihydropyranochromones as potential chemical scaffolds for antichagasic drug discovery

Bioactivity-guided isolation of trypanocidal coumarins and dihydro-pyranochromones from selected Apiaceae plant species

Sandhya R. Krishnan^a, Adrianna Skiba^b, Simon Vlad Luca^{c,d}, Laurence Marcourt^e, Jean-Luc Wolfender^e, Krystyna Skalicka-Woźniak^{a, b*}, Jürg Gertsch^{a*}

^a *Institute of Biochemistry and Molecular Medicine, University of Bern, Bern, Switzerland*

^b *Department of Chemistry of Natural Products, Medical University of Lublin, 20-093 Lublin, Poland*

^c *Biothermodynamics, TUM School of Life Sciences, Technical University of Munich, 85354 Freising, Germany*

^d *Department of Pharmacognosy, Grigore T. Popa University of Medicine and Pharmacy Iasi, 700115 Iasi, Romania*

^e *School of Pharmaceutical Sciences, University of Geneva, CMU, Rue Michel Servet 1, 1211 Geneva 4, Switzerland*

*corresponding authors: kskalicka@pharmacognosy; tel/fax: +48 81 448 7080; juerg.gertsch@unibe.ch; +41 31 684 41 24

Abstract

Bioactivity-guided isolation of natural products from plant matrices is widely used in drug discovery. Here, this strategy was applied to identify trypanocidal coumarins effective against the parasite *Trypanosoma cruzi*, the etiologic agent of Chagas disease (American trypanosomiasis). Previously, phylogenetic relationships of trypanocidal activity revealed a coumarin-associated antichagasic hotspot in the Apiaceae. In continuation, a total of 35 ethyl acetate extracts of different Apiaceae species were profiled for selective cytotoxicity against *T. cruzi* epimastigotes over host CHO-K1 and RAW264.7 cells at 10 $\mu\text{g/mL}$. A flow cytometry-based *T. cruzi* trypomastigote cellular infection assay was employed to measure toxicity against the intracellular amastigote stage. Among the tested extracts, *Seseli andronakii* aerial parts, *Portenschlagiella ramosissima* and *Angelica archangelica* subsp. *litoralis* roots exhibited selective trypanocidal activity and were subjected to bioactivity-guided fractionation and isolation by countercurrent chromatography. The khellactone ester isosamidin isolated from the aerial parts of *S. andronakii* emerged as a selective trypanocidal molecule (selectivity index ~ 9) and inhibited amastigote replication in CHO-K1 cells, though it was significantly less potent than benznidazole. The khellactone ester praeruptorin B and the linear dihydropyranochromones 3'-*O*-acetylhamaudol and ledebouriellol isolated from the roots of *P. ramosissima* were more potent and efficiently inhibited the intracellular amastigote replication at $< 10 \mu\text{M}$. The furanocoumarins imperatorin, isoimperatorin and phellopterin from *A. archangelica* inhibited *T. cruzi* replication in host cells only in combination, indicative of superadditive effects, while alloimperatorin was more active in fractions. Our study reports preliminary structure-activity relationships of trypanocidal coumarins and shows that pyranocoumarins and dihydropyranochromones are potential chemical scaffolds for antichagasic drug discovery.

Keywords: *Trypanosoma cruzi*; Chagas disease; Apiaceae; trypanocidal activity; bioactivity-guided fractionation; coumarins; pyranocoumarins; liquid-liquid chromatography

Journal Pre-proof

1. Introduction

Natural products are small molecules produced by secondary metabolism (hence called secondary or specialized metabolites) in large quantities in plants where they are thought to provide an evolutionary benefit (Maplestone et al., 1992; Williams, DA; Lemke, 2002). They offer high structural diversity and stereochemical content which render them attractive for early drug discovery (Stratton et al., 2015). Natural product research has significantly contributed to the chemotherapy of parasitic diseases such as quinine and the Nobel prize-winning artemisinin for treating malaria (Achan et al., 2011; Bridgford et al., 2018), among others.

Trypanosoma cruzi causes Chagas disease (CD) or American trypanosomiasis, a neglected tropical disease naturally transmitted by insect vectors and limited to Latin America (Pérez-Molina and Molina, 2018; Salm and Gertsch, 2019). Infectious diseases caused by protozoan parasites like *T. cruzi*, *Leishmania* sp., and *Plasmodium* sp. are responsible for considerable morbidity worldwide. There is an urgent need for safer and more efficacious therapies and vaccines for managing tropical parasitic diseases (Kratz, 2019). The currently available antichagasic drugs benznidazole and nifurtimox are suboptimal as they are not efficacious to treat chronic Chagas disease, pose a risk for resistance and can exert severe side effects (Ribeiro et al., 2020). Thus, the development of new and effective antichagasic drugs represents a unmet clinical need and a major challenge for drug discovery (Campos et al., 2014; Mejia et al., 2012). The Drugs for Neglected Diseases initiative's (DNDi's) states that an optimal early lead compound against trypanosomes must exhibit activity against parasites at $\leq 10 \mu\text{M}$ and have a 10-fold greater potency against parasites vs. mammalian cells (selectivity index, SI) (Ioset JR, Brun R, Wenzler T, Kaiser M, 2009).

In a previous study, we systematically profiled an antichagasic ethnopharmacology-inspired plant extract library from Bolivia and more comprehensively, general botanical drugs from the Mediterranean *De Materia Medica* unrelated to the use for the treatment of CD (Salm et al.,

2021). We uncovered two major antichagasic phylogenetic hotspots as potential entry points for drug discovery. The first phylobioactive anthraquinone cluster has been investigated and among the anthraquinones emodin (6-methyl-1,3,8-trihydroxyanthraquinone) was identified as an outstanding trypanocidal compound (Salm et al., 2021). The primary focus of the present study was to investigate the phylobioactive cluster related to plant taxa rich in coumarins (Salm et al., 2021). To efficiently identify active principles in complex plant mixtures, bioactivity-guided isolation (BAGI), also called bio-guided or bioassay-guided fractionation and isolation in principle provides a useful methodology to identify bioactive molecules (Pieters and Vlietinck, 2005). Herein, we present the results from the screening of selected plant species of the Apiaceae family, extensive bioactivity-guided fractionation, BAGI, and subsequent identification and testing of trypanocidal fractions and isolated compounds. Initially, ethyl acetate (EtOAc) extracts, containing semipolar to apolar molecules, were tested for selective toxicity against *T. cruzi*. Those EtOAc extracts presenting significant antitrypanosomal activity were then subjected to fractionation, with the aim to identify and characterize trypanocidal natural products, including coumarins. The selectivity of the extracts and bioactivity-guided fractions was verified by measuring differential cytotoxicity on *T. cruzi* epimastigotes and mammalian CHO-K1 cells. Moreover, the EtOAc extracts and bioactive fractions were tested in a fluorescence-activated cell scanning (FACS)-based parasite release assay, using GFP-expressing parasites, to assess their activity on amastigote replication in infected mammalian host cells.

Apiaceae (previously Umbelliferae) is one of the largest plant families composed of 466 genera and nearly 3800 species worldwide (Alvim et al., 2005). Although this family has yielded numerous pharmacologically active extracts and natural products, including those having broad antimicrobial properties (Albernaz et al., 2010; Coelho et al., 2019), few studies have investigated the trypanocidal activity against *T. cruzi* (Pereira et al., 2021; Rea et al., 2013;

Rodríguez-Hernández et al., 2019). Because coumarins (1,2-benzopyrone) are typically present in the Apiaceae, Rutaceae, and Asteraceae, in this study we focused on Apiaceae species which contain the broad spectrum of natural coumarin diversity that shaped the evolution of this family (Berenbaum, 2001). While synthetic coumarin derivatives like 3-carboxyamidocoumarins (Alvim et al., 2005), coumarin–chalcone hybrid (Vazquez-Rodriguez et al., 2013), 3-arylcoumarins (Robledo-O’Ryan et al., 2017), 4-methylamino-coumarins (Soares et al., 2019) and tricyclic coumarins (Coelho et al., 2019) have been reported to exert some antitrypanosomal activity, primarily on *T. cruzi* epimastigotes, there is a dearth of information regarding potential trypanocidal activity of naturally occurring coumarins. To date, primarily 4-substituted mammea-type coumarins isolated from the leaves of the tree *Calophyllum brasiliense* Cambess (Calophyllaceae) have been shown to exhibit potent trypanocidal activity similar to benznidazole against three Mexican strains of *T. cruzi* (Rodríguez-Hernández et al., 2019). This was based on an initial screening on *C. brasiliense* extracts (Albernaz et al., 2010). Simple coumarins with a fully substituted ring system, including the typical benzyl moiety at C4, displayed high selectivity for the parasites, i.e., they were not cytotoxic to the mammalian cells tested (Rodríguez-Hernández et al., 2019). Moreover, the untypical pyranocoumarin soulamarin has been shown to be effective against *T. cruzi* epimastigotes and amastigotes only at very high concentrations (>200 μ M) (Rea et al., 2013). Spurred by these promising previous findings, here we report a BAGI approach and identification of antichagasic coumarins and dihydropyranochromones, revealing hitherto unknown trypanocidal angular pyranocoumarins and linear dihydropyranochromones. Moreover, our study reveals apparent super-additive trypanocidal effects upon combining furanocoumarins and illustrates the inherent problem of shifting host cell cytotoxicity upon fractionation, which pose major challenges in BAGI, especially in long-term parasite infection assays. Based on these data, we provide a tangible starting point for future structure-activity

relationship (SAR) studies and follow-up investigations on antichagasic coumarins and dihydropyranochromones.

2. Results and discussion

2.1. Biological profiling of selected Apiaceae plant species

As shown in Table 1, a total of 35 EtOAc extracts belonging to 10 plant genera of the Apiaceae family were screened for selective trypanocidal effects at 10 $\mu\text{g/mL}$. This relatively low concentration was chosen to reduce the risk of identifying non-specific or weakly antitrypanosomal natural products. Since antichagasic molecules must readily cross the plasma membrane of the mammalian host cells to reach the intracellular amastigotes (Figure 1), extracts using polar solvents were avoided in this study as they would contain sugars, glycosylated or polyphenolic natural products, thus adding unnecessary complexity and skewing the mass/volume percent of inactive versus active molecules. Therefore, EtOAc provided an optimal solvent to include all semi-polar and more apolar secondary metabolites (Salm et al., 2021). First, we determined concentrations from the dried extract dissolved in DMSO resulting in 50% growth inhibition of both *T. cruzi* epimastigote (IC_{50}) and Chinese hamster ovary CHO-K1 cells (cytotoxicity, CC_{50}) (Table 1). Since the infective *T. cruzi* trypomastigotes do not replicate and amastigotes only replicate within the host cells, the epimastigote insect stage (Figure 1) is typically used to assess the selective toxicity (selectivity index, SI) over host cells in similarly proliferating cells *in vitro* over 72 h. Further, we assessed the pharmacologically relevant toxic effects of extracts on amastigotes in a cellular infection assay using a FACS-based parasite release assay at 15 $\mu\text{g/mL}$ (Table 1). In this assay, the trypomastigote-infected CHO-K1 cells were washed to remove remaining parasites after 24 h and the intracellular amastigote replication was determined after 5 days post-infection as number of released parasites (trypomastigotes and pre-maturely released amastigotes). These parasites were harvested from the extracellular medium of infected CHO-K1 cells at 5 days

post-infection, at which most host cells already burst to release the trypomastigotes (Figure 1). Effects on the amastigote replication process within the host cells could thus be determined quantitatively post-parasite release by FACS. Interestingly, the following extracts had no inhibitory effect on the growth of epimastigotes (the insect stage that replicates outside of cells) or CHO-K1 cells but did inhibit amastigote replication and thus reduced the amounts of parasites from infected cells (>75%): *Crithmum maritimum* L. (fruit), *Peucedanum alsaticum* L. (fruit), *Seseli elatum* subsp. *osseum* (Crantz) P.W.Ball (fruit), *Seseli pallasii* Besser (fruit) (Table 1). This may be due to specific effects on the host cells, e.g. host cell radical oxygen species (ROS) formation. Many Apiaceae species contain polyacetylenes like falcarinol and falcarindiol, which can increase ROS in mammalian host cells (Young et al., 2008) and could thus kill amastigotes indirectly disturbing the fine-tuned ROS homeostasis (Paula et al., 2020). We have previously shown that falcarindiol is a covalent inhibitor of cannabinoid CB1 receptors (Leonti et al., 2010), which has also been suggested to play a possible role in *T. cruzi* host cell infection (Croxford et al., 2005). A recent study on marine halophytes showed that sea fennel's (*C. maritimum*) flowers exert significant trypanocidal activity in which it was shown that falcarindiol was responsible for the trypanocidal activity against the *T. cruzi* Y and Sylvio X10/1 strains (Pereira et al., 2021).

As shown in Table 1, only few extracts exhibited selective cytotoxicity for *T. cruzi* (SI > 2) and reduced parasite host cell replication and release by more than 75% compared to the DMSO control: *Angelica amurensis* Schischk. (fruit), *Angelica archangelica* subsp. *litoralis* (Wahlenb.) Thell. (fruit), *Ferula kelleri* Koso-Pol. (root), *Portenschlagiella ramosissima* (Port.) Tutin (root), *Seseli andronakii* Woronow ex Schischk. (flower and inflorescences), *Seseli foliosum* (Sommier & Levier) Manden. (root), *Seseli leucospermum* Waldst. & Kit. (fruit), *Seseli rupicola* Woronow (fruit and inflorescences) and *Seseli transcaucasicum* (Schischk.) Pimenov & Sdobnina (root). The remaining plant extracts were strongly cytotoxic,

i.e., their respective CC_{50} values for CHO-K1 cells were less than the IC_{50} value for epimastigotes. These extracts were therefore not pursued further in this study. In fact, differential cytotoxicity caused a major challenge for the BAGI approach of antichagasic natural products. Interestingly, we did not observe that fractions became less toxic towards host cells and more toxic towards the parasite, indicative of superadditive antichagasic effects of natural products.

Taking into account the SI, which is considered to be critical, we performed bioactivity-guided fractionation of the aerial parts of *S. andronakii*, roots of *P. ramosissima*, fruits of *A. archangelica* subsp. *litoralis* and the fruits of *P. alsaticum*. In liquid chromatography high resolution mass (LC-HRMS/MS) spectra of the extracts different coumarin types like simple, pyrano, and furanocoumarins were noted. We next attempted to isolate coumarins with potential specific trypanocidal activity.

2.2. Bioactivity-guided fractionation of trypanocidal species

The EtOAc extracts of *S. andronakii*, *P. ramosissima*, *A. archangelica* subsp. *litoralis*, and *P. alsaticum* were subjected to fractionation using liquid-liquid chromatography (LLC). One-minute fractions were collected and subjected both to biological testing as well as phytochemical analysis. The LLC fractions were assayed at 10 $\mu\text{g/mL}$ against *T. cruzi* epimastigotes, CHO-K1 and/or RAW264.7 cells alone, and infected host cells to assess the trypanocidal activity. The differential toxicity against *T. cruzi* epimastigotes was determined (Figures 2-5). GFP-expressing trypomastigotes were employed for the infection of CHO-K1 cells and a more relevant mammalian host cell line, RAW264.7 cells (mouse macrophage cell line) was also adapted. Macrophages are the first line of defense in the tissue-specific immune response against *T. cruzi* (Telleria, J., and Tibayrenc, 2017). Therefore, fractions from *A. archangelica* subsp. *Litoralis* and *P. alsaticum* were tested on RAW264.7 cells for differential cytotoxicity and *T. cruzi* infection and parasite release. Additionally, the selectively

trypanocidal fractions (relative to CHO-K1 cells) from *S. andronakii* and *P. ramosissima* were also measured for cytotoxicity on RAW264.7 cells (Table S1, Table S2).

2.2.1. Fractionation of *Seseli andronakii* (aerial parts)

In comparison to CHO-K1 cells, all LLC fractions obtained from the *S. andronakii* EtOAc extract exhibited more potent toxicity against trypanosomes with a SI > 3 (Figure 2). The fractions with the highest SI (~9) in agreement with the criteria set by DNDi (Ioset JR, Brun R, Wenzler T, Kaiser M, 2009) were 25–29 and 103–108, respectively. Fractions 25–29 and 30–32 were identified as two pure pyranocoumarins, **isosamidin** (96% purity) and **pteryxin** (83% purity), respectively (Table S1). We did not assign the configuration at 3' and 4' for **pteryxin** in fractions 30-32, but based on NMR data it was the (-)-*cis* configuration. For subsequent testing we purchased racemic (+)-*trans* and (-)-*cis* **pteryxin** (PHL83899 from Sigma Aldrich, Switzerland). Racemic **pteryxin** did not significantly inhibit amastigote replication and parasite release from infected RAW264.7 cells at 10 μ M (data not shown). On the other hand, the khellactone ester **isosamidin**, which has the (-)-*cis* configuration, was trypanocidal and showed good selectivity (SI ~9). Although **isosamidin** was not very potent (IC₅₀ ~ 30 μ M), it efficiently and selectively inhibited amastigote replication in host cells (Table S1). Given the very high similarity between **pteryxin** and **isosamidin** (Figure 6), we cannot exclude that the stereochemistry is crucial for the activity. The LLC fractions 103–108 were identified as a mixture of *cis*-**3',4'-diseneciolyoxy-3'-4'-dihydroseselin** and **3'-seneciolyoxy,4'-angeloyoxy-3'-4'-dihydroseselin** which we did not purify further (see Materials and Methods 4.4.). The fractions were tested on RAW264.7 cells for cytotoxicity (Table S1). Since these fractions were relatively more cytotoxic towards RAW264.7 cells, they were examined on infected cells only at a concentration of 1 μ g/mL. None of the fractions inhibited the release of parasites from infected RAW264.7 cells at this low concentration (Table S1). Overall, bioactivity-guided fractionation of the *S. andronakii* extract was difficult

because the fractions were more cytotoxic on the host cell than the original extract, thus gradually losing selectivity. We assume that the selective trypanocidal activity in *S. andronakii* EtOAc extract is primarily caused by pyranocoumarins of the khellactone scaffold. Because pteryxin appeared to be less active than isosamidin, further detailed SAR studies taking into account the stereochemistry at 3' and 4' and the role of the acyl moieties in the esters for trypanocidal effects should be considered.

2.2.2. Fractionation of *Portenschlagiella ramosissima* (roots)

The LLC fractions obtained from *P. ramosissima* extract were screened at 10 µg/mL on epimastigotes and CHO-K1 cells. Since the isolated fractions were not toxic for CHO-K1 cells at 10 µg/mL, they were evaluated at the same concentration for their effects on amastigote replication, i.e. inhibition of parasite release from infected cells. A strong inhibitory effect was observed on amastigote replication in *T. cruzi*-infected CHO-K1 cells with fractions 17–21 to 51–60 (~70–100%) (Figure 3A). The additional LLC fractions 17–21 to 51–60 were also tested for cytotoxicity in RAW264.7 cells (Table S2). Interestingly, these fractions were more cytotoxic towards RAW264.7 cells compared to CHO-K1 cells (Table S2) and we therefore had to reduce the test concentrations. The most selective trypanocidal fraction 17–21 (scatter plot in Figure 3A) did not inhibit parasite replication in infected RAW264.7 cells at 1 µg/mL (Table S2). Higher concentrations could not be tested as the test substance should ideally have no cytotoxic effects on the host cells. This clearly showed the limitation of BAGI for the identification of trypanocidal coumarins. Nevertheless, two fractions, 28–32 and 51–60, inhibited parasite release from infected CHO-K1 cells and were therefore subjected to further purification (see Materials and Methods 4.5). The identity of the fractions was determined by mass spectrometry and NMR as follows: fractions 28–32 were a mixtures of **pteryxin** and **ledebouriellol**, while **3'-O-acetylhamaudol** was identified as the only molecule in fractions 51–60 (see Materials and Methods 4.5). The natural **pteryxin** from this fraction tested alone

did not inhibit the release of parasites from infected RAW264.7 cells at 10 μ M (see Section 2.2.1), suggesting that the activity observed with fractions 28–32 must arise from the linear dihydropyranochromone derivative **ledebouriellol**, or through a superadditive effect, similar to what was observed with furanocoumarins (see below). **Ledebouriellol** has been isolated previously also from fruits of *Pecuedanum alsaticum* (Skalicka-Woźniak et al., 2012). Because in this study we used the reversed phase mode in CC isolation we did not isolate this compound. The IC_{50} value of the similar dihydropyranochromone **3'-O-acetylhamaudol** on parasite release was determined to be 5.02 μ M (95% CI 4.08–5.65 μ M) in CHO-K1 host cells (Figure 3C). Although the IC_{50} value of **3'-O-acetylhamaudol** meets the criteria set by DNDi (Ioset JR, Brun R, Wenzler T, Kaiser M, 2009), (IC_{50} against parasite growth < 10 μ M), it is still higher than the IC_{50} value of the benzimidazole obtained in the same assay (0.7 μ M [95% CI = 0.5–1.0 μ M]) (Figure 3B). The linear dihydropyranochromone scaffold seems to be an attractive scaffold for future SAR studies as it is overall more selectively trypanocidal. Additionally, fractions 6–8 were found to be a mixture of **epoxypteryxin** and **alsaticol** and did not show any effect on *T. cruzi* epimastigotes or in the infection assay (Figure 3A). At 10 μ M, the angular pyranocoumarin **praeruptorin B** (obtained at 98% purity during elution-extrusion mode) inhibited amastigote replication in RAW264.7 cells by ~79% (78.7 ± 10.1), with an estimated IC_{50} value < 10 μ M. The khellactone ester **praeruptorin B** has been shown to exert effects on mammalian cells at similar concentrations. It is a fatty acid synthase inhibitor (Zheng et al., 2018) and is known to display anti-inflammatory effects by suppressing NF- κ B signaling (Yu et al., 2012).

2.2.3. Superadditive trypanocidal effects of furanocoumarins obtained from *Angelica archangelica* subsp. *litoralis*

The selective cytotoxicity of the LLC fractions obtained from *A. archangelica* subsp. *Litoralis* extract for *T. cruzi* relative to RAW264.7 cells was assessed. Fractions that inhibited the

viability of epimastigotes at 10 $\mu\text{g}/\text{mL}$ by more than 30% were subsequently tested on infected RAW264.7 cells, namely, Fr. 12–16, 17–27, 39–40, and 43–49 (Figure 4). LC-MS analyses revealed that fractions 47–55 were a clean mixture of **imperatorin**, **phellopterin**, and **alloimperatorin** in the ratio of 1:2:4. This mixture inhibited the parasite release by ~80% at 10 $\mu\text{g}/\text{mL}$ (Figure 4) and was the most interesting LLC fraction. Since **imperatorin** and **phellopterin** at 10 μM did not show any trypanocidal effect, we conclude that **alloimperatorin** is the most trypanocidal furanocoumarin in this fraction. Thus, the ether linkage in the butyl substituent seems to have a detrimental effect on the trypanocidal activity. Fractions 17–27 and 28–31 were determined to be a mixture of **isoimperatorin** and **phellopterin** in ratios 3.6:1 and 10:1, respectively (see Materials and Methods 4.6). These LLC fractions were less trypanocidal as the EtOAc extract but still had a significant impact on the replication of parasites in infected RAW264.7 cells (Table S3). Intriguingly, when tested independently, **imperatorin**, **isoimperatorin**, and **phellopterin** (each 10 μM) exhibited no trypanocidal activity in infected RAW264.7 cells. From these data, it is evident that compound mixtures exhibit a superadditive effects in fractions 17-27 and 28-31. Previously, three other *Angelica* species: *Angelica dahurica* (Hoffm.) Benth. & Hook.f. ex Franch. & Sav., *Angelica pubescens* f. *biserrata* R.H.Shan & C.Q.Yuan and *Angelica sinensis* (Oliv.) Diels (ethanolic extracts from roots) showed trypanocidal activity with EC_{50} values in the range of 14.5-19.4 $\mu\text{g}/\text{mL}$ (Schinella et al., 2002). From literature data, furanocoumarins were the assumed major antichagasic compounds in these extracts (Schinella et al., 2002).

2.2.4. Fractionation of *Peucedanum alsaticum* (fruit)

The fractionation of *P. alsaticum* fruit EtOAc extract was also hampered by increasing cytotoxicity for the host cells upon fractionation. Fractions 7, 8, 12–13 contained, among other minor angular pyranocoumarins and furanocoumarins, **ledebouriellol oxide**, **peucenidin** and **samidin** (see Materials and Methods 4.7). These coumarins were cytotoxic against RAW264.7

cells and lead to cell death at $>15 \mu\text{M}$ ($10 \mu\text{g/mL}$). As shown in Figure 5, fractions 14, 24–26, and 34 were not cytotoxic for host cells but only partially inhibited the release of parasites from infected cells at the same concentration ($\sim 50\text{--}70\%$). Overall, the BAGI approach to identify selective trypanocidal natural products again presented challenges like higher cytotoxicity and poor selectivity upon fractionation.

2.3. Determination of the trypanocidal activity of additional naturally occurring coumarins and emerging structure-activity relationships

Based on the previously published data (Rea et al., 2013; Rodríguez-Hernández et al., 2019) and the observed differential trypanocidal activity of different pyrano- and furanocoumarins in the active plant extracts in this study, we measured additional coumarins. At a test concentration of $10 \mu\text{M}$, the widespread coumarin metabolite **umbelliferone**, the angular furanocoumarin **angelicin** and the unsubstituted linear furanocoumarin **xanthotoxol**, as well as the linear pyranocoumarin **xanthyletin** and the angular pyranocoumarin **seselin** did not show significant effects on amastigote replication and parasite release in infected RAW264.7 cells (data not shown). Together, these results suggest that by comparing inhibition efficacy on amastigote replication in infected host cells at a concentration range of $5\text{--}30 \mu\text{M}$ it is possible to deduce and estimate preliminary structure-activity relationships (SAR). As shown in Figure 6A, the dihydropyranochromone scaffold appears to be promising as 3'-O-acetylhamaudol and ledebouriellol were potently trypanocidal while alsaticol was inactive, indicating that a bulky substituent in the saturated pyranring is detrimental for the activity. Based on the present preliminary data, a more systematic SAR study should be performed on the khellactone scaffold taking into account the absolute stereochemistry and modifications of the natural hemiterpene esters (Figure 6B). The fact that **praeruptorin B** is both potent and efficacious against *T. cruzi* suggest that the extended ring system in linear pyranocoumarins, as observed in trypanocidal anthraquinones (Salm et al., 2021), is not a prerequisite for activity. While

furanocoumarins are phototoxic and rather promiscuous in their activity in general, especially at higher micromolar concentrations (Bruni et al., 2019), their antichagasic effects observed in this study remain inconclusive. However, it appears that the alkyl ether linkage could reduce potency and/or efficacy (Figure 6C). At present, the most potent natural coumarins are the mammea-type coumarins from *C. brasiliense* (Figure 6D), though we could not test these compounds in our assays. Some mammea-type coumarins were more potent than benznidazole (Rodríguez-Hernández et al., 2019). Although soulamarin was reported to be effective against *T. cruzi*, it is not potent (Rea et al., 2013). In our hands, the most potent ($IC_{50} < 15 \mu M$) and promising antichagasic natural chemical scaffolds were dihydropyranochromenes and angular pyranocoumarins (Figure 6).

3. Conclusions

In continuation of the initial trypanocidal screening of 26 Apiaceae plant species (Salm et al., 2021) we conducted bioactivity-guided fractionation and BAGI on four selected antitrypanocidal crude EtOAc extracts. Although we identified antichagasic dihydropyranochromenes and pyranocoumarins, this approach was challenging as the differential cytotoxicity frequently changed upon fractionation and the host cell toxicity of the compounds impacted the infection assays. The loss of activity during BAGI is a frequent problem and possibly due to loss of synergistic activities between the individual molecules having different biophysical properties (Gertsch, 2011; Nothias et al., 2018). Although the crude extract of *P. alsaticum* was not cytotoxic for mammalian cells, upon fractionation all fractions exhibited general cytotoxicity. While data from the parasite release assay suggested direct trypanocidal effects, we cannot exclude additional effects on host cells. It is also possible that coumarins interfere with host cell pathways involved in parasite replication and evasion processes without killing host cells in these assays. We observed that a defined mixture of

furanocoumarins (imperatorin, phellopterin, and alloimperatorin) apparently acted in concert to potently and effectively inhibit parasite replication and/or release (~80% at 10 µg/mL) in infected mammalian cells. Intriguingly, when tested independently at 10 µM, the pure furanocoumarins did not exhibit matching trypanocidal activity, providing an interesting case of apparent super-additivity between natural products, though we did not investigate this in more detail. Systematically studying structure-activity relationships of dihydropyranochromenes and angular pyranocoumarins could be a starting point to explore and develop the trypanocidal potential of these natural chemical scaffolds, though the metabolic stability of khellactone derivatives is questionable (Jing et al., 2016) and would have to be assessed for in *in vivo* studies.

4. Materials and methods

4.1. Chemicals

Analytical grade n-hexane, ethyl acetate, and methanol were purchased from Avantor Performance Materials Poland S.A. (Gliwice, Poland), whereas LC grade methanol, acetonitrile, and formic acid were provided by J.T. Baker (Deventer, Netherlands). The tetrazolium salts 3-(4,5-dimethylthiazol-2-yl)-2,5-diphenyltetrazolium bromide or MTT and 2,3-bis-(2-methoxy-4-nitro-5-sulfophenyl)-2H-tetrazolium-5-carboxanilide or XTT were purchased from Sigma Aldrich (USA)/ Carl Roth GmbH (Germany) and Thermo Fisher Scientific/ Alfa Aesar, (United States), respectively. Neomycin was purchased from Sigma Aldrich (USA). Cell culture media RPMI-1640 and DMEM were purchased from Sigma Aldrich (United States) or Carl Roth GmbH (Germany). The coumarin standards: pteryxin, praeruptorin B, imperatorin, isoimperatorin, phellopterin, umbelliferone, angelicin, xanthotoxol, xanthyletin and seselin were obtained from Sigma Aldrich (United States), PhytoLab (Germany), and Adooq Bioscience (United States).

4.2. Apparatus

Liquid-liquid chromatography experiments (LLC) were carried out on a CPC from Gilson (Middleton, WI, USA), model CPC250, with a total column volume of 250 mL, a maximum rotation speed of 3000 rpm, maximum pressure drop of 100 bar and typical flow rate up to 15 mL/min. The CPC unit was connected to a preparative PLC2250 LC system from Gilson. Semi-preparative HPLC experiments were performed on a Hitachi LaChrom 7000 HPLC system (Hitachi Ltd., Tokyo, Japan) equipped with a D-7000 interface, L-7150 pump, L-7420 DAD detector, and Advantec SF-3120 fraction collector. Analytical HPLC-DAD analyses were carried out on a Shimadzu 20A series HPLC (Shimadzu, Tokyo, Japan) coupled with a DGU-20A 3R automatic degasser, LC-20AD quaternary pump, SIL-20A HT auto-sampler, and SPD-M20A DAD detector. An Agilent 1200 HPLC system (Agilent Technologies, Santa Clara, CA, USA) equipped with a G1329A auto-sampler, G1379B degasser, G1312C binary pump, G1316B column oven, G1315B DAD detector, and G6530B Q-TOF mass spectrometer was used for the HPLC-DAD-ESI-QTOF-MS/MS investigations. A Bruker Avance Neo 600 MHz NMR spectrometer (Bruker BioSpin, Rheinstetten, Germany) supplied with a QCI 5 mm Cryoprobe and a SampleJet automated sample changer was employed for the NMR analyses.

4.3. Preparation of EtOAc extracts

The plant parts of selected Apiaceae plants were collected from the Botanical Garden of Maria Curie-Skłodowska University (UMCS, Lublin, Poland) and authenticated by a specialist. The dried and grounded plant material (50 g) was extracted with EtOAc (500 mL) for 48 h at room temperature. . After filtration and solvent removal, the crude extracts were obtained. The plant voucher numbers and yield of extraction are specified in Table 1.

The extracts were then fractionated by LLC on the CPC250 unit. The suitable biphasic solvent system needed for the LLC fractionation was selected through a series of shake-flask experiments with various mixtures of hexane/EtOAc/methanol/water (HEMWat). The partition

coefficients of the prominent peaks detected in the HPLC-DAD chromatograms were used as screening parameters. The partition coefficients were calculated as the ratio between the area of a certain peak in the upper phase divided by the area of the same peak in the lower phase. The solvent system that provided partition coefficient values for the main HPLC-DAD peaks between 0.2 and 5 (Ito, 2005) was chosen. Isolation parameters were selected separately for each extract. The structure of isolated compounds was confirmed by ESI-QTOF-MS/MS and NMR analyses: 1D NMR ($^1\text{H-NMR}$; $^{13}\text{C-DEPTQ-NMR}$) and 2D NMR (correlation spectroscopy, COSY; heteronuclear multiple-bond correlation, HMBC; multiplicity-edited heteronuclear single-quantum correlation, edited-HSQC; rotating-frame Overhauser enhancement spectroscopy, ROESY).

4.4. Fractionation of *Seseli andronakii*

The aerial parts of *Seseli andronakii* Woronow ex Schischk. (voucher no. 10/2019) were extracted using EtOAc, as mentioned in Section 4.3. Following extraction, 0.97 g of crude extract (yield 1.94%) was obtained. The HEMW at 2/1/2/1 (v/v/v/v), was selected for fractionation of the extract (Fig. S1). The LLC fractionation experiment was performed under the following conditions: operating modes – descending mode for 95 min followed by elution extrusion mode for 15 min, rotation speed – 1700 rpm, flow rate – 9 mL/min, injection volume – 10 mL, sample concentration – 7 mg/mL (dissolved in lower phase); UV wavelength – 254 nm (Fig. S2). A total number of 110 fractions (each of 9 mL) were collected and analyzed by HPLC-DAD. Fractions showing a similar chromatographic profile were pooled together and subjected to biological profiling (Section 4.10–4.12).

Two pure compounds were isolated (Fig. S3), namely **isosamidin** (2.88 mg, purity 96%, in fractions 25-29), **pteryxin** (1.87 mg, purity 83%, in fractions 30-32) as well as the mixture of **cis-3',4'-diseneciolyoxy-3'-4'-dihydroseselin** and **3'-seneciolyoxy,4'-angeloyloxy-3'-4'-**

dihydroseselin (2.42 mg, in fractions 103-108). The spectrometric data of the isolated compounds is summarized in the Supplementary Information (Fig. S4 — Fig. S24).

4.5. Fractionation of *Portenschlagiella ramossima*

The roots of *Portenschlagiella ramossima* (Port.) Tutin. (voucher no. 11/2019) were extracted using EtOAc, as mentioned in Section 4.3. After extraction, 5.48 g of crude extract (yield 10.96%) was obtained (Fig. S25). The solvent system HEMWat 3/2/3/2 (v/v/v/v), was selected. The LLC fractionation experiment was performed under the following conditions: operating modes – descending mode for 95 min followed by elution extrusion EE mode for 15 min, rotation speed – 1700 rpm, flow rate – 9 mL/min, injection volume – 10 mL, sample concentration – 40 mg/mL (dissolved in lower phase); UV wavelength – 254 nm (Fig. S26). A total number of 60 fractions (each of 9 mL) (plus 15 fractions of EE mode) were collected and analyzed by HPLC-DAD. Fractions showing a similar chromatographic profile were pooled together and subjected to biological profiling (Section 4.10–4.12).

Two pure compounds were isolated (Fig. S27), **3'-O-acetylhamaudol** (6.6 mg, purity 98.5%, fractions 51-60) and **praeruptorin B** (4.6 mg, purity 98%, EE mode). In addition, fractions 28-32 contained a mixture of two compounds, which were further purified by semi-preparative HPLC. The following conditions were used: column – Cosmosil C18-AR-II (250 × 10 mm, 5 μm); mobile phase: water (A), methanol (B); elution conditions – isocratic 70%B; flow rate – 2.5 mL/min; injection volume – 50 μL. Thus, two compounds were isolated, namely **pteryxin** (0.73 mg, purity 82%) and **ledebouriellol** (1.06 mg, purity 90%).

Additionally, a mixture of two compounds: **epoxypteryxin** and **alsaticol** (4.1 mg, fractions 6-8) were obtained. This fraction was inactive (Figure 3).

The structure of isolated compounds was confirmed by ESI-QTOF-MS/MS and NMR analyses and the spectrometric data is summarized in the Supplementary Information (Fig. S28 — Fig. S55).

4.6. Fractionation of *Angelica archangelica* subsp. *litoralis*

The fruits of *Angelica archangelica* subsp. *litoralis* (Wahlenb.) Thell. (voucher no. 12/2019) Following extraction, 5.92 g of crude extract (yield 11.84%) was obtained. The partition coefficients of the main peaks detected in the HPLC-DAD chromatogram of the *A. archangelica* extract (Fig. S56) were used as screening parameters. The solvent system HEMWat 2/1/2/1 (v/v/v/v), was selected. The LLC fractionation experiment was performed under the following conditions: operating modes – descending mode for 90 min followed by elution extrusion mode for 15 min, rotation speed – 1700 rpm, flow rate – 6 mL/min, injection volume – 10 mL, sample concentration – 35 mg/mL (dissolved in lower phase); UV wavelength – 254 nm (Fig. S57). A total number of 70 fractions (each of 6 mL) were collected and analyzed by HPLC-DAD. Fractions showing a similar chromatographic profile were pooled together and subjected to *Trypanosoma* assay (Section 4.10–4.12). After that the active fractions were checked for purity and the compounds within the fractions were identified by ESI-QTOF-MS/MS as follow:

- (fraction 17-27, 22.32 mg) mixture of **isoimperatorin** and **phellopterin** in ratio: 3.6:1 (based on HPLC area).
- (fraction 28-31, 2.07 mg) mixture of **imperatorin**, **phellopterin** and **alloimperatorin** (fraction 47-55, 3.27 mg) in ratio: 1:2:4 (based on HPLC area) (Fig. S58).

4.7. Fractionation of *Peucedanum alsaticum*

The fruits of *Peucedanum alsaticum* (voucher no. 13/2019) were extracted with EtOAc (500 mL) for 48 h at room temperature, and 315 mg of crude extract (yield 0.3%) were obtained. The partition coefficients of the main peaks detected in the HPLC-DAD chromatogram of the *P. alsaticum* extract (Fig. S59 – HPLC chromatogram of raw extract) were used as screening parameters. The solvent system HEMWat 6/5/6/5 (v/v/v/v), was selected. The LLC fractionation experiment was performed under the following conditions: operating modes –

descending mode for 90 min followed by elution extrusion mode for 15 min, rotation speed – 1700 rpm, flow rate – 6 mL/min, injection volume – 10 mL, sample concentration – 27 mg/mL (dissolved in lower phase); UV wavelength – 254 nm. A total number of 53 fractions (each of 6 mL) were collected and analyzed by HPLC-DAD. Fractions showing a similar chromatographic profile were pooled and subjected to biological profiling (Section 4.10–4.12). After that the active fractions were checked for purity and the compounds (Fig. S60) within the fractions were identified by ESI-QTOF-MS/MS as follows:

- (fraction 7 and 8, 1.08 mg and 1.15 mg, respectively) containing **ledebouriellol oxide** as the main compound.
- (fraction 12-13, 1.15 mg) containing mixture of **samidin** and **peucenidin**.
- (fraction 14, 0.96 mg) containing **peucenidin** as the main compound.
- (fraction 24-26, 0.96 mg) containing **ledebouriellol** as the main compound.
- (fraction 34, 0.29 mg) containing **notopterol** as the main compound (Fig. S59).

4.8. Mammalian cell culture

Chinese hamster ovarian cells CHO-K1 (ATCC® CCL-61™) and mouse macrophage cells RAW264.7 (ATCC® TIB-71™) were cultured in RPMI-1640 medium (Sigma Aldrich, MO, USA/ Carl Roth GmbH, Germany) supplemented with heat-inactivated fetal bovine serum (hiFBS, Sigma Aldrich, MO) at 37 °C in a humid atmosphere with 5% CO₂. Chinese hamster lung fibroblasts (ATCC® CCL-39™) transfected with empty pCDNA3.1 plasmid were cultured in DMEM medium supplemented with 10% hiFBS and 400 µg/mL G418.

4.9. Trypanosoma cruzi culture

Epimastigotes of *T. cruzi*, Y strain (ATCC® 50832™), were maintained in weekly passages in liver infusion tryptose (LIT) medium supplemented with 10% hiFBS at 28 °C as described previously (Salm et al., 2021). Epimastigote cultures in the logarithmic growth phase (1-5x10⁷ parasites/mL) were used for experiments unless mentioned otherwise. GFP overexpressing

epimastigotes were generated by transfection with pTREX-n-eGFP, a gift from Rick Tarleton (Addgene plasmid # 62544; <http://n2t.net/addgene:62544>; RRID:Addgene_62544) as described previously. GFP-expressing epimastigotes were cultured in LIT medium supplemented with 10% hiFBS and 500 µg/mL G418.

Metacyclic trypomastigotes were obtained from stationary phase epimastigotes using triatomine artificial urine (TAU) medium as described by Salm, et al. (Salm et al., 2021).

Trypomastigotes were harvested from the extracellular medium of CHO-K1 cells infected with metacyclic forms. The trypomastigotes were maintained by weekly passages in CHO-K1 cells and collected from culture supernatants at 5 days post-infection (dpi) by centrifuging at 2000 x g for 15 min. The trypomastigotes were then allowed to swim out of the pellet by incubating the 2 mL of the residual medium at 37 °C for 2 h. Alternatively, empty vector-transfected CCL-39 cells were used for maintaining GFP-expressing trypomastigotes.

All experiments involving live *T. cruzi* were performed in the BSL-3* lab approved by the safety authorities of the University and Canton of Bern, Switzerland: The Standard Operational Procedures of the experiments were reported to the Swiss Authority Federal Office of Public Health (BAG).

4.10. *Host cell cytotoxicity assessment*

Cytotoxicity or antiproliferative effects of coumarin extracts, CPC fractions, and pure coumarins on mammalian cells was assessed using MTT as described previously (Salm et al., 2021). CHO-K1 cells or RAW264.7 cells were used for screening the compounds. Briefly, the cells were seeded at a density of 2000/well in 96 well plates (TPP AG, Switzerland). After 24 h of incubation at 37 °C, 5% CO₂, plant extracts, and fractions or compounds (prepared in DMSO) were added to the cells. In all experiments, solvent controls were included, and the final DMSO concentration was below 0.5%. The extracts or fractions were screened at a single concentration of 10 µg/mL or six concentrations ranging from 100 µg/mL to 0.8 µg/mL. After

72 h, the plates were examined under an inverted microscope for sterility and growth of controls after the incubation period. The spent medium was removed, and 100 μ L of fresh medium containing 0.5 mg/mL final concentration of MTT was added to the cells. The plates were incubated for 4 h at 37 $^{\circ}$ C, 5% CO₂. The formazan crystals were solubilized by adding 200 μ L of DMSO and mixed thoroughly. The absorbance was determined at 550 nm using a Tecan plate reader. The values were corrected to the blank medium and solvent control (DMSO only). Results were expressed as percentage cell viability relative to solvent control or IC₅₀ values estimated by GraphPad Prism version 8.0. Each assay was performed in technical triplicates in at least two independent experiments.

4.11. Trypanocidal activity

As per the DNDi, an ideal lead compound must exhibit activity against trypanosomes at a concentration ≤ 10 μ M and have a 10-fold greater potency against *T. cruzi* vs. mammalian cells (SI)(Ioset JR, Brun R, Wenzler T, Kaiser M, 2009). To assess the selectivity, the trypanocidal activity against epimastigotes was assessed by XTT as described previously (Salm et al., 2021). Briefly, 1.5×10^5 epimastigotes were seeded per well in 96 well plates. The plant extracts or compounds was added at a single concentration of 10 μ g/mL (for screening experiments) or six concentrations ranging from 100 μ g/mL to 0.8 μ g/mL (for IC₅₀ determination; in case of pure compounds, 100 μ M to 0.8 μ M) for 72 h at 28 $^{\circ}$ C. In all the experiments, benznidazole was used as the positive control. Following the incubation period, the plates were examined under the microscope for sterility and growth of controls. To the plates, 50 μ L of XTT and PMS (Phenazine methosulfate, Sigma Aldrich, MO, USA) solution (XTT and PMS at 0.5 mg/mL and 0.025 mg/mL, respectively) was added, and the plates were then incubated at 28 $^{\circ}$ C for 2.5 h. The parasites were fixed by the addition of 50 μ L of methanol for 15 min before measuring the absorbance at 490 nm on a Tecan plate reader. Results were expressed as percentage cell viability relative to vehicle control or IC₅₀ values calculated by GraphPad Prism

version 8.0. All assessments were performed in triplicates in at least two independent experiments.

4.12. *FACS-based quantitation of released parasites from infected cells*

The host cells, CHO-K1, and RAW264.7 cells, were seeded in 24 well plates at a density of 40,000 cells and 10,000 cells/mL, respectively. The cells were allowed to adhere for 24 h and infected with trypomastigotes harvested by the swim-out procedure described above at a multiplicity of 10. On the next day, non-internalized trypomastigotes were washed away, and fresh RPMI with 0.5% or 2% FBS (for CHO-K1 cells and RAW264.7 cells) was added to the wells along with the test substance. In all experiments, the screening was performed in triplicate, including a DMSO control and benznidazole control at 20 μ M. The released parasites were fixed using 4% paraformaldehyde in PBS for 1 h and the samples were then analyzed using FACScan (BD Biosciences) as described previously (Salm et al., 2021). At least two independent experiments in triplicates were performed to determine the activity of the substances at 10 μ g/mL and 15 μ g/mL in the case of fractions and extracts, or 10 μ M for pure compounds.

Declaration of competing interest

The authors declare that they have no competing financial interests or personal relationships that could have influenced the work or conclusions reported in this study.

Data availability

Data will be made available on request.

Acknowledgements

We would like to thank Mr. Jaroslaw Widelski from the Department of Pharmacognosy, Medical University of Lublin, for helping in the preparation of extracts.

Appendix B. Supplementary data

Supplementary data to this article can be found online at ...

References

- Achan, J., Talisuna, A.O., Erhart, A., Yeka, A., Tibenderana, J.K., Baliraine, F.N., Rosenthal, P.J., D'Alessandro, U., 2011. Quinine, an old anti-malarial drug in a modern world: role in the treatment of malaria. *Malar. J.* 10, 144. <https://doi.org/10.1186/1475-2875-10-144>
- Albernaz, L.C., de Paula, J.E., Romero, G.A.S., Silva, M. do R.R., Grellier, P., Mambu, L., Espindola, L.S., 2010. Investigation of plant extracts in traditional medicine of the Brazilian Cerrado against protozoans and yeasts. *J. Ethnopharmacol.* 131, 116–121. <https://doi.org/10.1016/j.jep.2010.06.011>
- Alvim, J., Dias, R.L.A., Castilho, M.S., Oliva, G., Corrêa, A.G., 2005. Preparation and evaluation of a coumarin library towards the inhibitory activity of the enzyme gGAPDH from *Trypanosoma cruzi*. *J. Braz. Chem. Soc.* 16, 763–773. <https://doi.org/10.1590/S0103-50532005000500014>
- Berenbaum, M.R., 2001. Chemical mediation of coevolution: Phylogenetic evidence for Apiaceae and associates. *Ann. Missouri Bot. Gard.* 88, 45–59. <https://doi.org/10.2307/2666131>
- Bridgford, J.L., Xie, S.C., Cobbold, S.A., Pasaje, C.F.A., Herrmann, S., Yang, T., Gillett, D.L., Dick, L.R., Ralph, S.A., Dogovski, C., Spillman, N.J., Tilley, L., 2018. Artemisinin kills malaria parasites by damaging proteins and inhibiting the proteasome. *Nat. Commun.* 2018 91 9, 1–9. <https://doi.org/10.1038/s41467-018-06221-1>
- Bruni, R., Barreca, D., Protti, M., Brighenti, V., Righetti, L., Anceschi, L., Mercolini, L., Benvenuti, S., Gattuso, G., Pellati, F., 2019. Botanical Sources, Chemistry, Analysis, and

- Biological Activity of Furanocoumarins of Pharmaceutical Interest. *Molecules* 24, 2163.
<https://doi.org/10.3390/MOLECULES24112163>
- Campos, M.C., Leon, L.L., Taylor, M.C., Kelly, J.M., 2014. Benznidazole-resistance in *Trypanosoma cruzi*: Evidence that distinct mechanisms can act in concert.
<https://doi.org/10.1016/j.molbiopara.2014.01.002>
- Coelho, G.S., Andrade, J.S., Xavier, V.F., Sales Junior, P.A., Rodrigues de Araujo, B.C., Fonseca, K. da S., Caetano, M.S., Murta, S.M.F., Vieira, P.M., Carneiro, C.M., Taylor, J.G., 2019. Design, synthesis, molecular modelling, and in vitro evaluation of tricyclic coumarins against *Trypanosoma cruzi*. *Chem. Biol. Drug Des.* 93, 337–350.
<https://doi.org/10.1111/CBDD.13420>
- Croxford, J.L., Wang, K., Miller, S.D., Engman, D.M., Tyler, K.M., 2005. Effects of cannabinoid treatment on Chagas disease pathogenesis: Balancing inhibition of parasite invasion and immunosuppression. *Cell. Microbiol.* 7, 1592–1602.
<https://doi.org/10.1111/j.1462-5822.2005.00577.x>
- Gertsch, J., 2011. Botanical drugs, synergy, and network pharmacology: forth and back to intelligent mixtures. *Planta Med.* 77, 1086–1098. <https://doi.org/10.1055/S-0030-1270904>
- Ioset, J.R., Brun, R., Wenzler, T., Kaiser, M., Yardley V., 2009. Drug screening for kinetoplastid diseases: A training manual for screening in neglected diseases. DNDi Pan-Asian Screening Network, April 2009: 74pp.
- Ito, Y., 2005. Golden rules and pitfalls in selecting optimum conditions for high-speed counter-current chromatography. *J. Chromatogr. A* 1065, 145–168.
<https://doi.org/10.1016/J.CHROMA.2004.12.044>
- Jing, W., Liu, R. Du, W., Luo, Z., Guo, P., Zhang, T., Zeng, A., Chang, C., Fu, Q., 2016. Pharmacokinetic and Metabolic Characteristics of Herb-Derived Khellactone Derivatives,

- A Class of Anti-HIV and Anti-Hypertensive: A Review. *Molecules* 21, 314.
- Kratz, J.M., 2019. Drug discovery for chagas disease: A viewpoint. *Acta Trop.* 198. <https://doi.org/10.1016/J.ACTATROPICA.2019.105107>
- Leonti, M., Casu, L., Raduner, S., Cottiglia, F., Floris, C., Altmann, K.H., Gertsch, J., 2010. Falcarinol is a covalent cannabinoid CB1 receptor antagonist and induces pro-allergic effects in skin. *Biochem. Pharmacol.* 79, 1815–1826. <https://doi.org/10.1016/J.BCP.2010.02.015>
- Maplestone, R.A., Stone, M.J., Williams, D.H., 1992. The evolutionary role of secondary metabolites — a review. *Gene* 115, 151–157. [https://doi.org/10.1016/0378-1119\(92\)90553-2](https://doi.org/10.1016/0378-1119(92)90553-2)
- Mejia, A.M., Hall, B.S., Taylor, M.C., Gómez-Palacio, A., Wilkinson, S.R., Triana-Chávez, O., Kelly, J.M., 2012. Benznidazole-Resistance in *Trypanosoma cruzi* Is a Readily Acquired Trait That Can Arise Independently in a Single Population. *J. Infect. Dis.* 206, 220. <https://doi.org/10.1093/INFDIS/JIS331>
- Nothias, L.F., Nothias-Esposito, M., Da Silva, R., Wang, M., Protsyuk, I., Zhang, Z., Sarvepalli, A., Leyssen, P., Touboul, D., Costa, J., Paolini, J., Alexandrov, T., Litaudon, M., Dorrestein, P.C., 2018. Bioactivity-Based Molecular Networking for the Discovery of Drug Leads in Natural Product Bioassay-Guided Fractionation. *J. Nat. Prod.* 81, 758–767. <https://doi.org/10.1021/ACS.JNATPROD.7B00737>
- Paula, J.I.O., Pinto, J. da S., Rossini, A., Nogueira, N.P., Paes, M.C., 2020. New perspectives for hydrogen peroxide in the amastigogenesis of *Trypanosoma cruzi* in vitro. *Biochim. Biophys. acta. Mol. Basis Dis.* 1866, 165951–165951. <https://doi.org/10.1016/J.BBADIS.2020.165951>
- Pereira, C.G., Moraes, C.B., Franco, C.H., Feltrin, C., Grougnet, R., Barbosa, E.G., Panciera, M., Correia, C.R.D., Rodrigues, M.J., Custódio, L., 2021. In Vitro Anti- *Trypanosoma*

- cruzi Activity of Halophytes from Southern Portugal Reloaded: A Special Focus on Sea Fennel (*Crithmum maritimum* L.). *Plants* (Basel, Switzerland) 10, 2235 <https://doi.org/10.3390/PLANTS10112235>
- Pérez-Molina, J.A., Molina, I., 2018. Chagas disease. *Lancet* 391, 82–94. <https://doi.org/10.1097/01.JAA.0000547749.92933.6a>
- Pieters, L., Vlietinck, A.J., 2005. Bioguided isolation of pharmacologically active plant components, still a valuable strategy for the finding of new lead compounds? *J. Ethnopharmacol.* 100, 57–60. <https://doi.org/10.1016/J.JEP.2005.05.029>
- Rea, A., Tempone, A.G., Pinto, E.G., Mesquita, J.T., Rodrigues, E., Silva, L.G.M., Sartorelli, P., Lago, J.H.G., 2013. Soulmamarin Isolated from *Calophyllum brasiliense* (Clusiaceae) Induces Plasma Membrane Permeabilization of *Trypanosoma cruzi* and Mitochondrial Dysfunction. *PLoS Negl. Trop. Dis.* 7. <https://doi.org/10.1371/JOURNAL.PNTD.0002556>
- Ribeiro, V., Dias, N., Paiva, T., Hagström-Bex, L., Nitz, N., Pratesi, R., Hecht, M., 2020. Current trends in the pharmacological management of Chagas disease. *Int. J. Parasitol. Drugs Drug Resist.* 12, 7. <https://doi.org/10.1016/J.IJPDDR.2019.11.004>
- Robledo-O’Ryan, N., Moncada-Basualto, M., Mura, F., Olea-Azar, C., Matos, M.J., Vazquez-Rodriguez, S., Santana, L., Uriarte, E., Moncada-Basualto, M., Lapier, M., Maya, J.D., 2017. Synthesis, antioxidant and antichagasic properties of a selected series of hydroxy-3-aryl coumarins. *Bioorg. Med. Chem.* 25, 621–632. <https://doi.org/10.1016/J.BMC.2016.11.033>
- Rodríguez-Hernández, K.D., Martínez, I., Agredano-Moreno, L.T., Jiménez-García, L.F., Reyes-Chilpa, R., Espinoza, B., 2019. Coumarins isolated from *Calophyllum brasiliense* produce ultrastructural alterations and affect in vitro infectivity of *Trypanosoma cruzi*. *Phytomedicine* 61, 152827. <https://doi.org/10.1016/J.PHYMED.2019.152827>

- Salm, A., Gertsch, J., 2019. Cultural perception of triatomine bugs and Chagas disease in Bolivia: a cross-sectional field study. *Parasit. Vectors* 12, 291. <https://doi.org/10.1186/s13071-019-3546-0>
- Salm, A., Krishnan, S.R., Collu, M., Danton, O., Hamburger, M., Leonti, M., Almanza, G., Gertsch, J., 2021. Phylobioactive hotspots in plant resources used to treat Chagas disease. *iScience* 24, 102310. <https://doi.org/10.1016/J.ISCI.2021.102310>
- Schinella, G.R., Tournier, H.A., Prieto, J.M., Ríos, J.L., Buschiazzo, H., Zaidenberg, A., 2002. Inhibition of *Trypanosoma cruzi* growth by medical plant extracts. *Fitoterapia* 73, 569–575. [https://doi.org/10.1016/S0367-326X\(02\)00246-0](https://doi.org/10.1016/S0367-326X(02)00246-0)
- Skalicka-Woźniak, K., Mroczek, T., Garrard, I., Głowniak, K., 2012. Isolation of the minor and rare constituents from fruits of *Peucedanum alsaticum* L. using high-performance counter-current chromatography. *J. Sep. Sci.* 35, 790–797. <https://doi.org/10.1002/JSSC.201100815>
- Soares, F.G.N., Goëthel, G., Kagami, L.P., Das Neves, G.M.H., Sauer, E., Birriel, E., Varela, J., Gonçalves, I.L., Von Poser, G., González, M., Kawano, D.F., Paula, F.R., De Melo, E.B., Garcia, S.C., Cerecetto, H., Eifler-Lima, V.L., 2019. Novel coumarins active against *Trypanosoma cruzi* and toxicity assessment using the animal model *Caenorhabditis elegans*. *BMC Pharmacol. Toxicol.* 20. <https://doi.org/10.1186/S40360-019-0357-Z>
- Stratton, C.F., Newman, D.J., Tan, D.S., 2015. Cheminformatic comparison of approved drugs from natural product versus synthetic origins. *Bioorg. Med. Chem. Lett.* 25, 4802–4807. <https://doi.org/10.1016/J.BMCL.2015.07.014>
- Telleria, J., and Tibayrenc, M., 2017. American Trypanosomiasis. Chagas Disease: One Hundred Years of Research. Elsevier Inc.
- Vazquez-Rodriguez, S., Figueroa-Guñez, R., Matos, M.J., Santana, L., Uriarte, E., Lapier, M., Maya, J.D., Olea-Azar, C., 2013. Synthesis of coumarin–chalcone hybrids and evaluation

of their antioxidant and trypanocidal properties. *Medchemcomm* 4, 993–1000.

<https://doi.org/10.1039/C3MD00025G>

Williams, DA; Lemke, T., 2002. Chapter 1. Natural products, in: *Principles of Medicinal Chemistry*. Philadelphia: Lippincott Williams Wilkins., p. 25.

Young, J.F., Christensen, L.P., Theil, P.K., Oksbjerg, N., 2008. The Polyacetylenes Falcarinol and Falcarindiol Affect Stress Responses in Myotube Cultures in a Biphasic Manner. *Dose-Response* 6, 239. <https://doi.org/10.2203/DOSE-RESPONSE.08-008.YOUNG>

Yu, P.J., Jin, H., Zhang, J.Y., Wang, G.F., Li, J.R., Zhu, Z.G., Tian, Y.X., Wu, S.Y., Xu, W., Zhang, J.J., Wu, S.G., 2012. Pyranocoumarins isolated from *Peucedanum praeruptorum* Dunn suppress lipopolysaccharide-induced inflammatory response in murine macrophages through inhibition of NF- κ B and STAT3 activation. *Inflammation* 35, 967–977. <https://doi.org/10.1007/S10753-011-9400-Y>

Zheng, Z.G., Lu, C., Thu, P.M., Zhang, X., Li, H.J., Li, P., Xu, X., 2018. Praeruptorin B improves diet-induced hyperlipidemia and alleviates insulin resistance via regulating SREBP signaling pathway. *RSC Adv.* 8, 354–366. <https://doi.org/10.1039/C7RA11797C>

Figure legend

Figure 1. Biology of *T. cruzi* epimastigote, the insect vector form in Triatominae, and trypomastigote/amastigote in host cell stages. In this study we performed two assays that measure epimastigote toxicity (assay I) and inhibition of amastigote replication within the host cell/trypomastigote release using a GFP-expressing *T. cruzi* (assay II).

Figure 2. Differential toxicity of fractions isolated from aerial parts of *Seseli andronakii* on *T. cruzi* epimastigotes and CHO-K1 cells at 10 μ g/mL. The toxicity on amastigotes quantified as inhibition of parasite release from trypomastigote infected CHO-K1 cells upon treatment with

all the fractions is summarized in the table. The blue symbols in the scatter plot indicate fractions that completely inhibited parasite release from infected cells at 10 $\mu\text{g/mL}$. Data represent mean values \pm SD from at least two independent experiments each performed in triplicate. See also Supplementary Table S1.

Figure 3. Trypanocidal profiling of fractions isolated from roots of *Portenschlagiella ramosissima*. (A) The cytotoxic effects of the fractions were tested on *T. cruzi* epimastigotes and CHO-K1 cells at 10 $\mu\text{g/mL}$. The blue symbols denote fractions with selective trypanocidal activity. The toxicity on amastigotes quantified as inhibition of parasite release from trypomastigote infected CHO-K1 cells was evaluated at 10 $\mu\text{g/mL}$ and is summarized. Data represent mean \pm SD from at least two independent experiments each performed in triplicate. (B–C) Dose-dependent inhibition of parasite release from infected CHO-K1 cells by (B) benznidazole and (C) **3'-O-acetyl-hamaudol**. Data represent mean values \pm SD from three independent experiments each performed in triplicate. See also Supplementary Table S2.**Figure 4.** Differential toxicity of isolated fractions from *A. archangelica* subsp. *litoralis* fruits on *T. cruzi* epimastigotes and RAW264.7 cells at 10 $\mu\text{g/mL}$. Fractions that inhibited epimastigote growth by more than 30% (indicated by blue symbols in the scatter plot) were subsequently tested on infected RAW264.7 cells. The results are summarized in the table. Data represent mean values \pm SD from two independent experiments performed in triplicate. See also Supplementary Table S3.

Figure 5. Differential toxicity of fractions isolated from fruits of *Peucedanum alsaticum* on *T. cruzi* epimastigotes and RAW264.7 cells at 10 $\mu\text{g/mL}$. The fractions 14, 24–26, and 34, which did not inhibit the growth of RAW264.7 cells, were tested for inhibitory effects on epimastigotes (indicated by blue symbols in the scatter plot). The inhibition of amastigote

replication and parasite release by the fractions is summarized in the table. Data represent mean values \pm SD from two independent experiments performed in triplicate. See also Supplementary Table S3.

Figure 6. Summary of current knowledge on antichagasic natural coumarin scaffolds (red) and derivatives and first preliminary structure-activity relationships. (A) dihydropyranochromenes, (B) angular pyranocoumarins, (C) furanocoumarins, (D) published natural antichagasic coumarins.

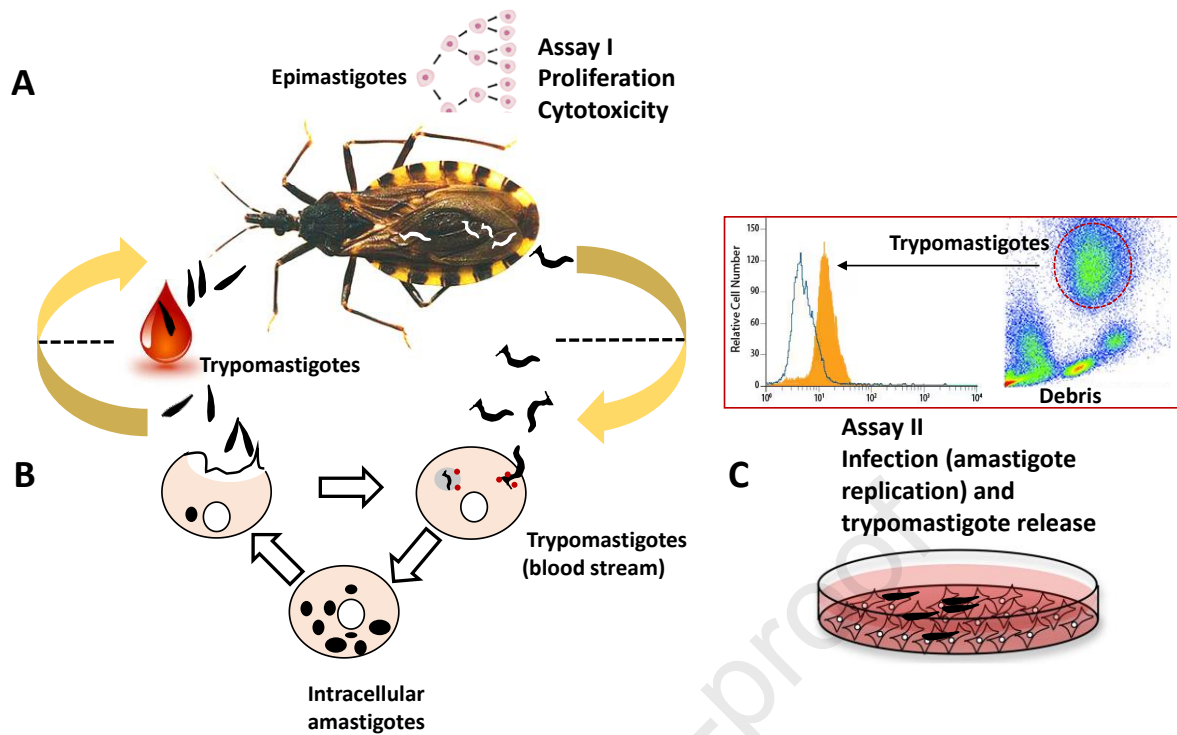
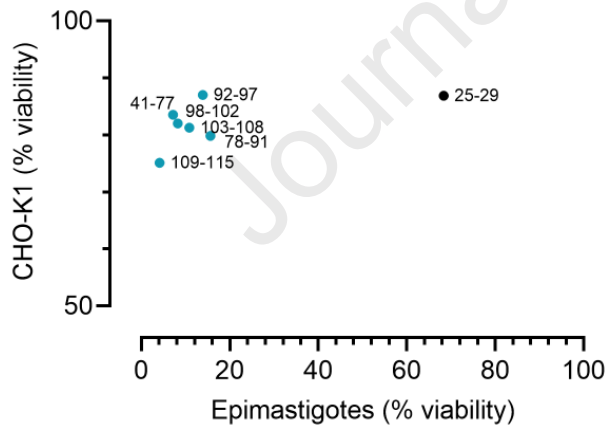


Figure 1.



Fraction ID	Inhibition of parasite replication in RAW264.7 cells at 10 µg/mL (% of vehicle control)
25-29 Isosamidin	65.9 ± 18.5
41-77	100
78-91	100
92-97	100
98-102	100
103-108	100
109-115	100

Figure 2.

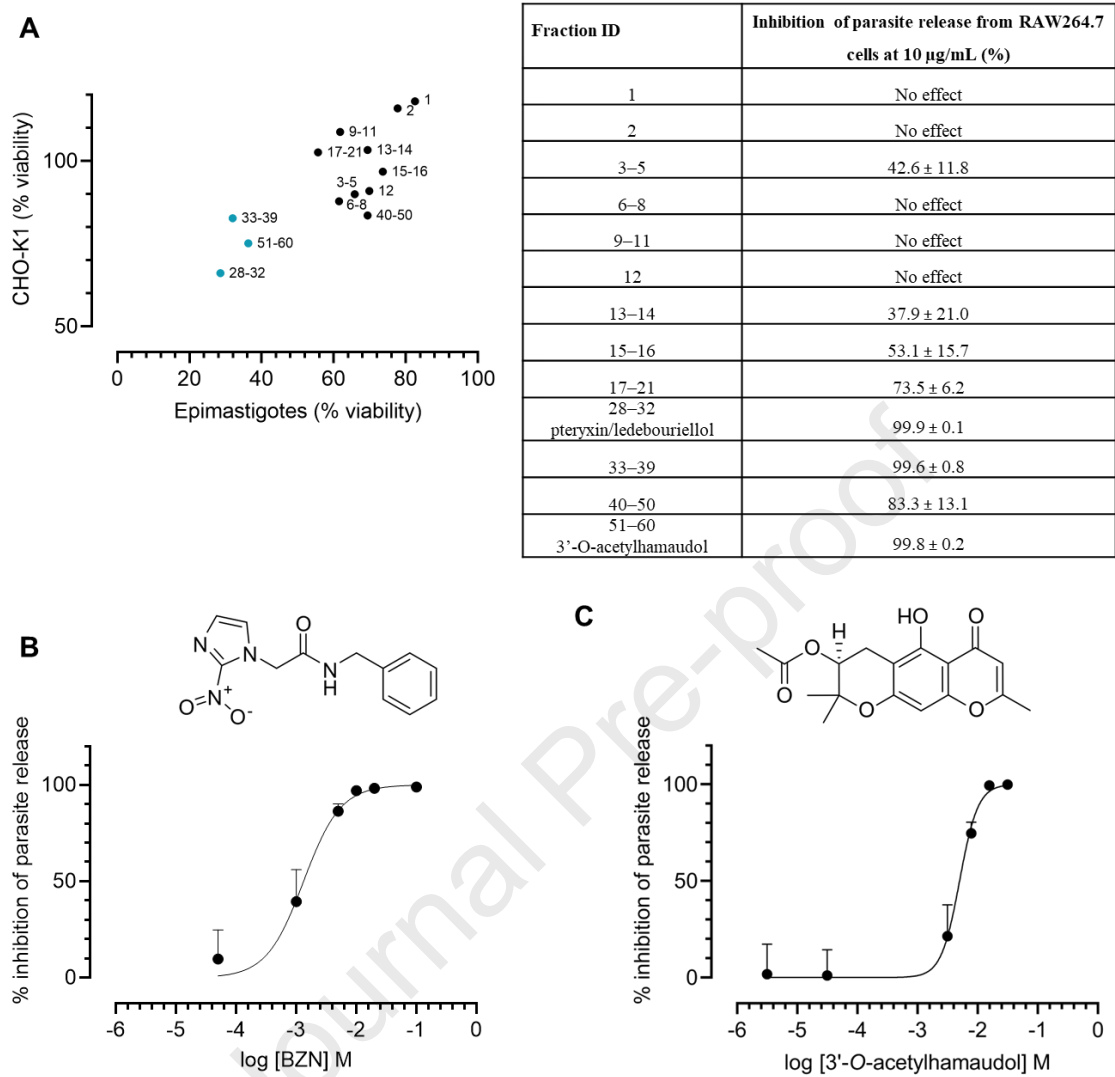


Figure 3.

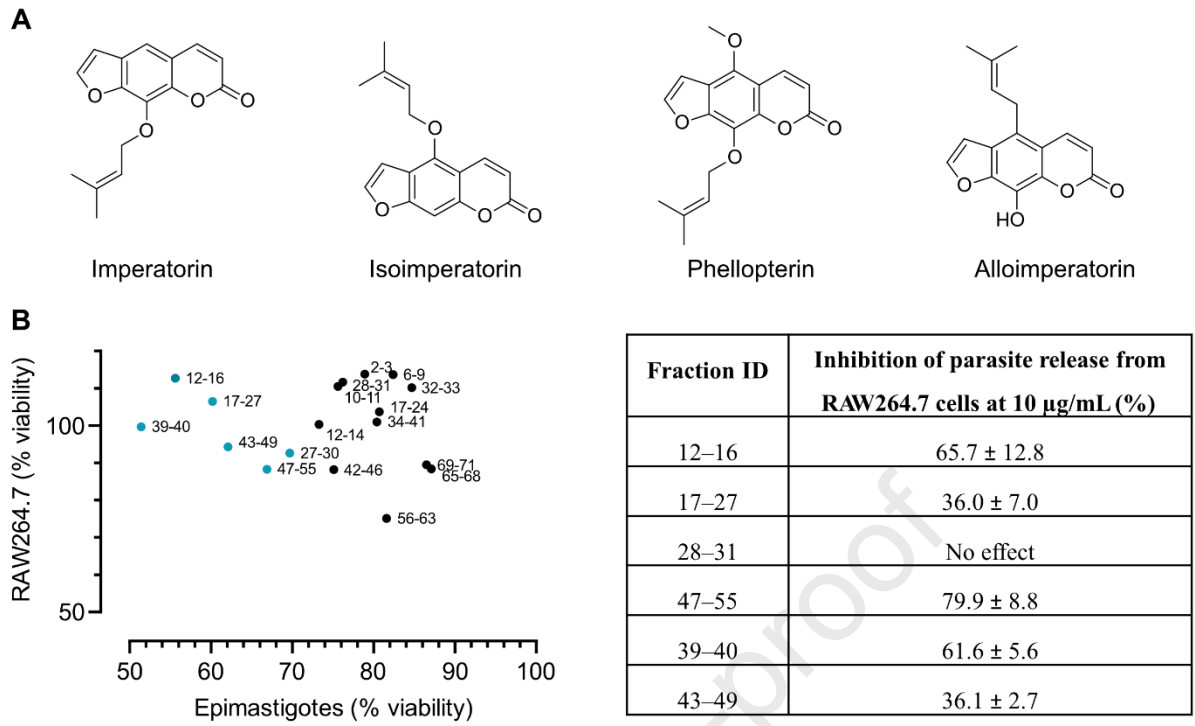


Figure 4.

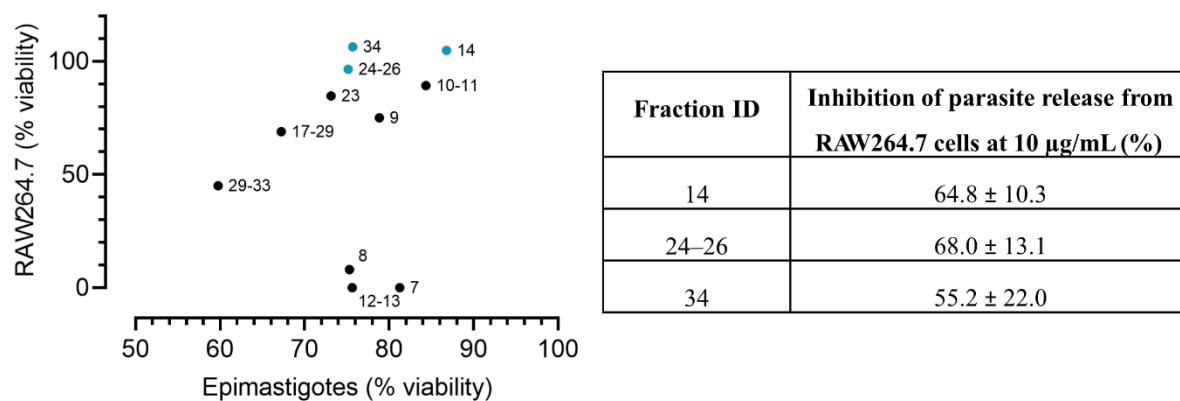


Figure 5.

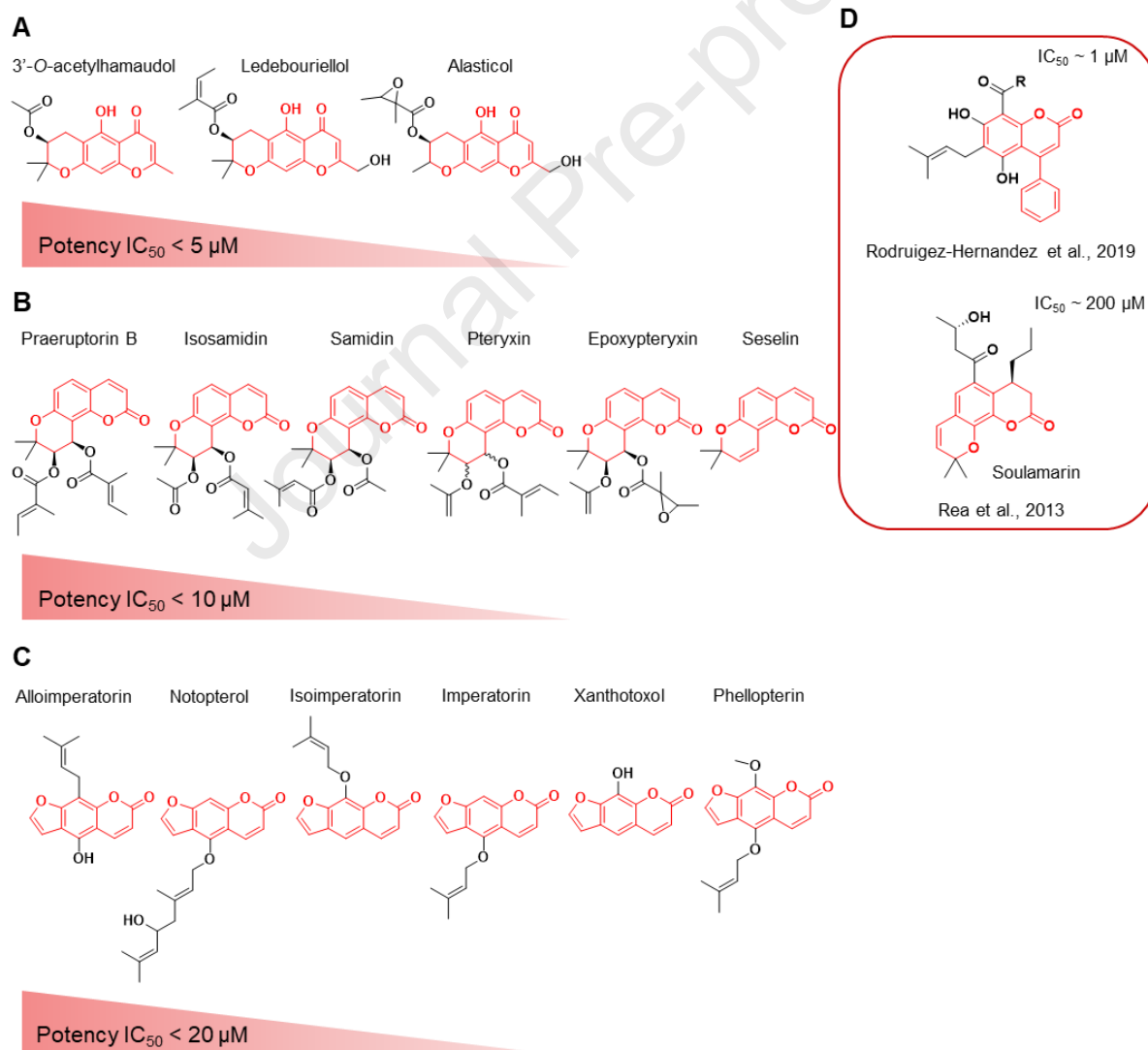


Figure 6.

Table 1. Cytotoxicity of EtOAc plant extracts for <i>T. cruzi</i> epimastigotes and CHO-K1 cells. The IC ₅₀ and CC ₅₀ values were determined over a range of 100–0.8 µg/mL after 72 h. The inhibitory activity on parasite release was tested at 15 µg/mL using a FACS-based assay at six days post-infection. Data represent mean ± SD from three independent experiments performed in triplicate. Plant species	Plant part	CC₅₀ CHO-K1 cells (µg/mL)	IC₅₀ epimastigotes (µg/mL)	% Inhibition amastigote replication (parasite release) at 15 µg/mL
Benznidazole (control)	-	>100 µM	7.8 ± 0.5 µM	99.3 ± 0.4 ^a
<i>Angelica archangelica</i> subsp. <i>litoralis</i> (Wahlenb.) Thell.	Fruit	78.3 ± 3.6	30.6 ± 6.5	79.7 ± 20.0
<i>Aegopodium podagraria</i> L.	Herb	n.d	n.d	97.4 ± 0.8
<i>Angelica amurensis</i> Schischk.	Fruit	>100	32.2 ± 17.7	88.6 ± 8.0
<i>Angelica lucida</i> L.	Fruit	55.7 ± 13.6	>100	57.4 ± 22.8
<i>Crithmum maritimum</i> L.	Fruit	>100	>100	76.6 ± 13.0
<i>Ferula akitschkensis</i> B.Fedtsch. ex Koso-Pol.	Root	22.5 ± 0.5	11.4 ± 5.8	97.9 ± 2.2
<i>Ferula kelleri</i> Koso-Pol.	Root	34.9 ± 5.9	10.7 ± 5.1	100.1 ± 0.7
<i>Heracleum sphondylium</i> L.	Fruit	49.7 ± 3.2	>100	No effect
<i>Ligusticum scoticum</i> L.	Fruits	>100	71.4 ± 19.3	21.4 ± 20.7
<i>Orlaya grandiflora</i> (L.) Hoffm.	Fruit	>100	>100	22.9 ± 15.6
<i>Peucedanum alsaticum</i> L.	Fruit	>100	>100	79.9 ± 7.3
<i>Peucedanum luxurians</i> Tamamsch.	Fruit	54.6 ± 1.8	58.4 ± 21.6	56.1 ± 12.3
	Aerial part	43.1 ± 9.9	>100	91.5 ± 4.2
<i>Peucedanum schottii</i> Besser ex DC.	Fruit	>100	>100	15.5 ± 8.1
<i>Peucedanum verticillare</i> Spreng.	Fruit	63.1 ± 4.1	42.8 ± 12.4	83.1 ± 19.1
<i>Portenschlagiella ramosissima</i> (Port.) Tutin	Root	>100	52.1 ± 11.4	81.3 ± 17.7

<i>Seseli andronakii</i> Woronow ex Schischk.	Flowers and umbels	43.6 ± 9.5	25.9 ± 3.5	83.7 ± 16.7
	Fruit	>100	>100	68.8 ± 19.0
	Aerial part	28.0 ± 5.4	7.6 ± 4.3	99.2 ± 1.6
<i>Seseli buchtormense</i> W.D.J.Koch	Aerial part	47.9 ± 1.5	33.9 ± 13.6	93.8 ± 4.8
<i>Seseli devenyense</i> Simonk.	Fruit	>100	>100	18.9 ± 28.8
<i>Seseli elatum</i> subsp <i>osseum</i> (Crantz) P.W.Ball	Fruit	>100	>100	88.6 ± 15.4
	Aerial part	21.4 ± 3.1	47.3 ± 14.5	91.5 ± 5.5
<i>Seseli foliosum</i> (Sommier & Levier) Manden.	Fruit	13.0 ± 0.8	31.4 ± 21.8	93.5 ± 7.3
	Aerial part	19.9 ± 1.7	17.7 ± 3.1	93.5 ± 7.3
	Root	47.4 ± 0.6	17.3 ± 5.8	99.4 ± 1.1
<i>Seseli leucospermum</i> Waldst. & Kit.	Fruit	>100	27.2 ± 1.9	92.0 ± 4.8
<i>Seseli libanotis</i> W.D.J.Koch	Fruit	>100	>100	40.6 ± 34.2
	Aerial part	41.8 ± 5.6	45.8 ± 19.7	85.4 ± 15.1
<i>Seseli montanum</i> L.	Fruit	55.7 ± 5.6	>100	97.5 ± 1.4
	Aerial part	40.6 ± 7.2	58.5 ± 19.6	80.2 ± 23.4
<i>Seseli pallasii</i> Besser	Fruit	>100	>100	89.4 ± 12.5
<i>Seseli rupicola</i> Woronow	Inflorescences and fruits	69.1 ± 3.5	30.8 ± 19.0	92.9 ± 6.5
<i>Seseli transcaucasicum</i> (Schischk.) Pimenov & Sdobnina	Aerial part	34.6 ± 8.7	18.6 ± 4.5	98.1 ± 2.2
	Root	42.7 ± 9.1	11.7 ± 6.2	99.1 ± 0.9

Blue-shaded rows indicate extracts that are selective for *T. cruzi* and were subject to bioactivity-guided fractionation. Extracts with similar selectivity for *T. cruzi* are in grey-shaded rows.

^a Benznidazole, positive control was tested at 20 µM.

- Biological profiling of 35 extracts of Apiaceae species for trypanocidal effects
- Bioguided fractionation and isolation showing superadditive effects
- Antichagasic potential of both pyranocoumarins and dihydropyranochromones

Journal Pre-proof

Declaration of interests

The authors declare that they have no known competing financial interests or personal relationships that could have appeared to influence the work reported in this paper.

The authors declare the following financial interests/personal relationships which may be considered as potential competing interests:

Prof. Jurg Gertsch ic co-guest editor of this Special Issue

Journal Pre-proof